

Designing Squirrel Cage Rotor Slots with High Conductivity

James L. Kirtley Jr.

Massachusetts Institute of Technology
Cambridge, Massachusetts, 02139, USA

Tel: +1 617 253 2357 Fax: +1 617 258 6774 email: kirtley@mit.edu

Abstract: This paper describes an investigation into ways of taking advantage of the higher conductivity of cast copper in rotors of induction motors. Deep bar and multiple cage effects are useful in design of such machines. It is shown that a useful understanding of how different slot shapes work may be developed through the use of frequency response curves that describe rotor slot impedance as a function of rotor frequency. Good starting, running and stray loss characteristics can be identified in such frequency response curves.

I. INTRODUCTION:

There has been, in recent years, an effort to make cast copper rotors for industrial use induction motors. The objective is to make motors more efficient because of the higher conductivity of copper. In addition, the reduced losses in such motors may lead to better design flexibility and therefore motors that are more compact.

In this paper we examine the tradeoff between running efficiency and starting performance. In order to understand how induction motors work it is necessary to have a good model for the conduction properties of the conductors in the slots of the rotor. We employ a simple model that has been developed for this purpose.¹ We propose to examine the frequency response of the rotor bar impedance for indications of how the motor will work, taking into account not only running efficiency and starting performance but also stray load losses which are also affected by rotor bar impedance.

II. ROTOR IMPEDANCE

For illustration, Fig. 1 shows a comparison of torque vs. speed for two identical notional induction motors, differing only in the value of rotor resistance, commonly noted as R_2 . The characteristic curve with higher resistance would, for all load torques, operate at a somewhat lower running speed (and hence higher slip and lower efficiency) than the

machine with the lower resistance. On the other hand, starting torque is lower for the low resistance rotor and this might lead to unsatisfactory performance in some applications.

The use of copper as the conductor of induction motor rotors would typically lead to improvements in efficiency, relative to motors using aluminum. This is often done in large motors in which squirrel cages are fabricated from bars of material brazed to end rings. In such machines it is common to employ 'starting' bars of higher resistivity material. Our objective here, however, is to discuss ways of designing rotor slots for fabrication by casting a single material, as is commonly done with aluminum as the rotor conductor material.

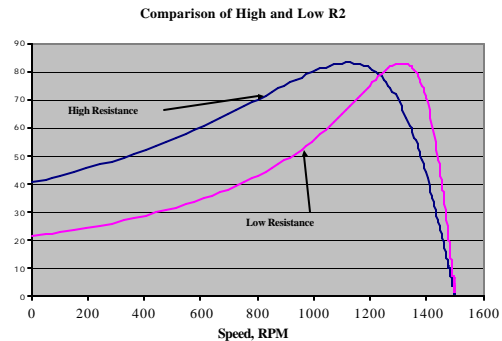


Figure 1: Notional Torque Speed Curves

In some induction motors, what is called the 'deep bar' effect, or distribution of rotor currents due to eddy currents, is taken advantage of. When the rotor is stationary or turning slowly the frequency of rotor currents is relatively high, the currents crowd to the top of the rotor bar and the resistive part of impedance is relatively high.

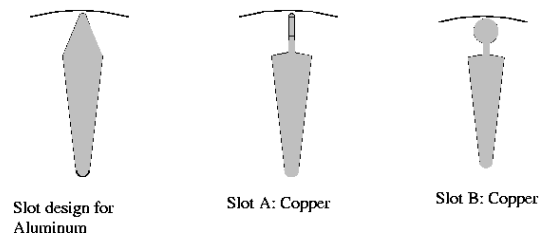


Figure 2: Comparison of Slot Shapes

Shown in Fig. 2 are three different possible slot shapes. On the left is the shape used in the original cast aluminum rotor. It has a characteristic tapered shape so that the teeth between rotor bars are of uniform section. It tapers toward the rotor surface.

Fig. 3 shows the real and reactive parts of the impedance of the slot designed for aluminum with two different materials: aluminum and copper.

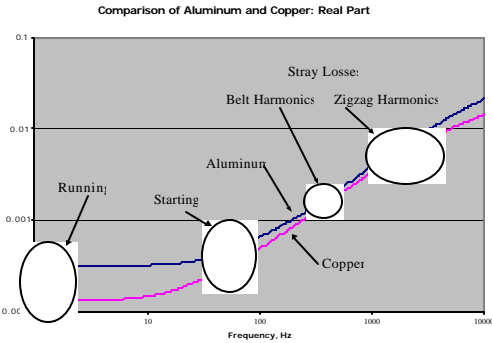


Figure 3: Aluminum and Copper Slot Resistance

The frequency range shown in Fig. 3 encompasses not only starting and running frequencies, but also the frequencies of currents in the rotor bars due to the various space harmonics of the stator winding. As can be seen in the figure, the copper rotor has substantially lower resistance over the whole frequency range, but the difference is largest at running conditions. At higher frequencies the smaller skin depth of copper causes the impedance of those bars to increase.

Now the question at hand is this: Can we shape the rotor bars to take advantage of the higher conductivity of copper to produce good running efficiency and yet have satisfactory starting performance? We do not believe we have found the optimum bar shape yet, but we can at least illustrate the question with a comparison of the other two bar shapes shown in Fig. 2. Fig. 4 shows a comparison of the slot resistance of those two bars over the same frequency range.

The first copper bar was designed with a narrow top within which the relatively high frequency currents of starting flow, producing a higher resistance at start. Note that this is only partially successful, as the second bar design, B actually results in larger resistance at starting. This is because the narrow slot between the top, starting

bar and the rest of the conductor is effective at isolating starting frequency currents to the starting bar. At the same time, note that Bar A results in higher resistance at harmonic frequencies, indicating possibly higher stray load losses.

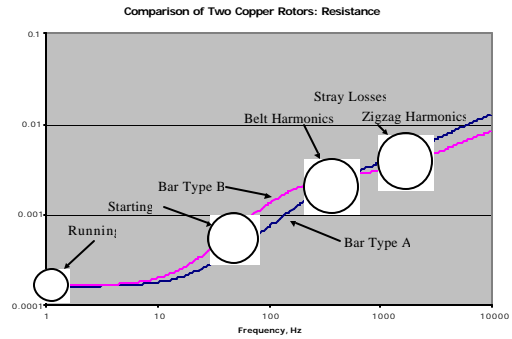


Figure 4: Comparison of two copper rotors (Slot A and Slot B of Fig. 2)

III METHODOLOGY

Induction motors are represented for the purpose of design analysis by an equivalent circuit as shown in Fig. 5.ⁱⁱ Some components of the rotor leakages and resistances of each section are frequency dependent and therefore functions of rotor frequency and so speed.

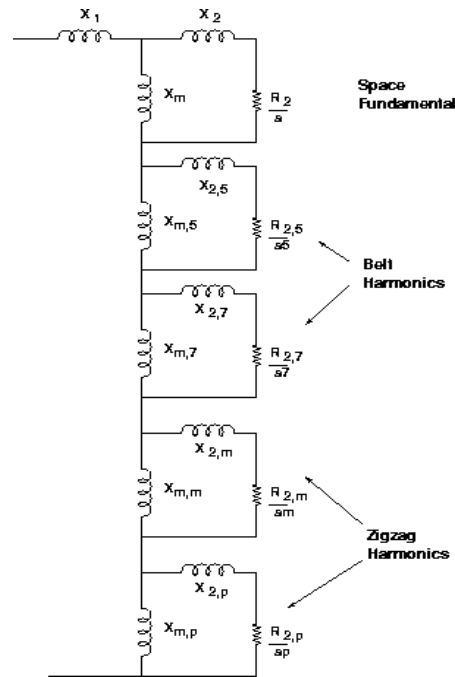


Figure 5 'Alger' Equivalent Circuit Model

To establish rotor resistances and reactances we use a simple technique for representing the rotor bar as a ladder network. The bar is divided into a relatively large number of slices, oriented in a direction perpendicular to the rotor surface. Each such slice is represented by a simple 'tee' circuit consisting of inductance, representing cross-slot flux and resistance, representing the current carried by that part of the slot.

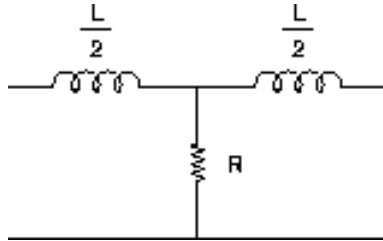


Figure 6: Element Model

To find the values of the slot parameters make reference to Figure 7.

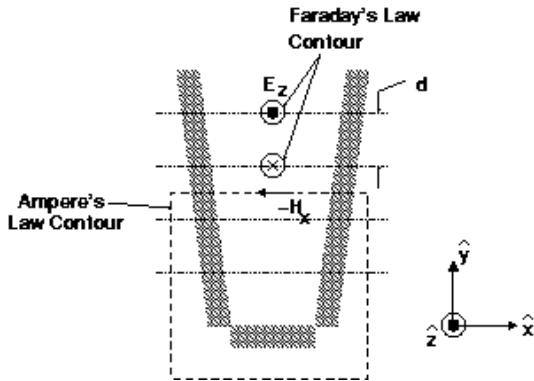


Figure 7 Illustration of calculation of slot parameters

Note that, from the Ampere's Law contour shown, magnetic field crossing the slot at some vertical position y is related to all current in the slot below that position. From the Faraday's Law contour we see that all of the inductance elements in the slot are in series and the electric field (voltage per unit length) driving current is the sum of voltages across all inductive elements below the position y . Then if we represent the slot as a series connection of basic 'tee' elements, the inductance per unit length of a section is:

$$L = \frac{\mu_0 d}{w(y)} \quad (1)$$

where d is the height of the section and w is width of the slot at that position. Resistance per unit length is:

$$R = \frac{1}{\sigma d w(y)} \quad (2)$$

where σ is material conductivity.

The tee elements are accordingly connected together as is shown in Fig. 8.

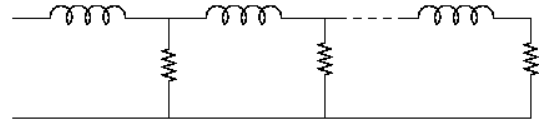


Figure 8: Ladder representation of slot impedance

A more sophisticated technique might have been used. A good example of this is the elegant formulation of Williamson using a finite element model for each slot embedded in a circuit model of the machine as shown in Fig. 5ⁱⁱⁱ. In this case it was felt that the accuracy achieved by the ladder network would probably be sufficient, and the resulting efficiency of calculation makes it possible to draw some conclusions regarding optimization of the machine.

IV SLOT REPRESENTATION

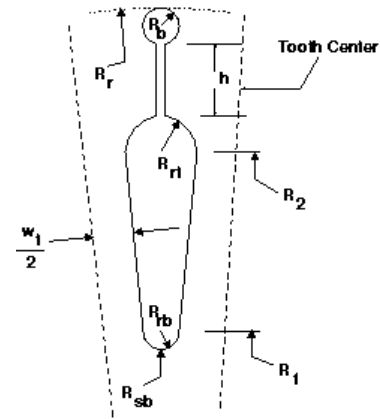


Figure 9: Slot Geometry

For this discussion, we adopt a canonical slot geometry as is shown in Fig. 9. The 'main' part of the slot is a trapezoid that is narrower at the bottom than at the top to allow for constant width of teeth between slots. The top and bottom part of the slot is bounded by semicircles of appropriate radius. The 'leakage slot has radial height h and the starting bar has radius R_b . If we define the slot factor to be the ratio of slot width to slot pitch (slot plus tooth) at the top of the trapezoidal (main) part of the slot to be:

$$I_s = \frac{2R_{rt}N_R}{2pR_2} \quad (3)$$

Then the radius of that top part of the rotor slot is $R_2 = R_r - 2R_b - h - R_{st}$, Where there are N_R rotor slots, R_r is the rotor radius, h is the height of the leakage slot, R_{st} is the radius of the upper semicircle (twice the slot width at that radius) and R_b is the radius of the starting bar.

We adopt the convention that the radius of the bottom of the slot to the top of the main slot section is $R_{rb} = f_r R_{rt}$. The slot tooth width is:

$$w_t = \frac{2pR_0}{N_r} \quad (4)$$

where the radius R_0 is where the slot width (the width of the trapezoid) would go to zero:

$$R_0 = R_2(1 - I_s) \quad (5)$$

Now, to find the radius R_2 , we observe that:

$$2N_R R_{rt} = 2pR_2(1 - I_s) \quad (6)$$

Which when combined with the earlier expression yields:

$$R_2 = \frac{R_r - 2R_b - h}{1 + \frac{p(1 - I_s)}{N_R}} \quad (7)$$

The radius of the bottom of the trapezoidal section is $R_1 = R_2(1 + f_r)(1 - I_s)$. And the radius of the slot bottom is $R_{sb} = R_1 - R_{rb}$. Note that the slot geometry is fully defined by R_r , N_R , f_r , λ_s , R_b and h .

V. EXAMPLE MACHINE

To illustrate the impact of using copper in a machine we adopt a 5.5 kW, 50 Hz machine built for pump application so that starting torque is an important feature. The rotor slot we assume here is similar to the slot in the actual machine (in which the starting bar is not exactly cylindrical as we assume. The bar is defined by a starting bar diameter of 4.2 mm, a leakage slot that is 3 mm high and 1 mm wide, 28 rotor bars in a rotor that is 110 mm in diameter and a ratio of inner to maximum slot widths of $f_r = 0.5$. The slot as constructed is shown in Fig. 10. The horizontal lines represent section widths.

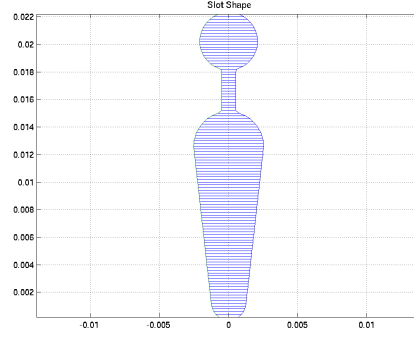


Figure 10: Example Slot Shape

Using standard analysis techniques and the slot impedance estimation technique described here, we can estimate machine performance for cast aluminum and cast copper. The analysis technique has been compared with the actual 5.5 kW motor and the results are reasonably accurate for both copper and aluminum rotor cages. The frequency response for the two conductors is shown in Fig. 11 and the Torque-speed curves are shown in Fig. 12.

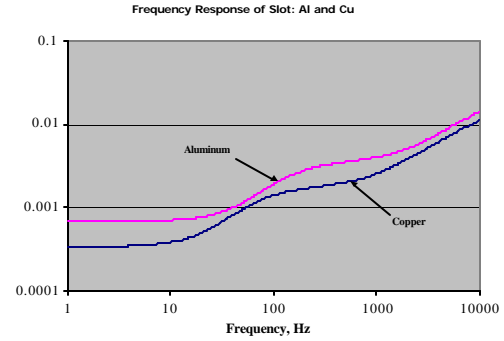


Figure 11 Frequency Response Comparison: Aluminum Vs. Copper

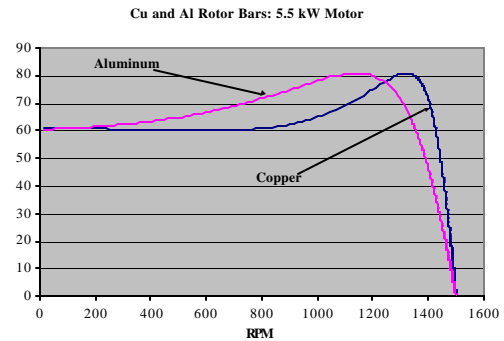


Figure 12: Comparison of copper vs. aluminum in 5.5 kW motor

In this machine the copper rotor achieves better performance by taking advantage of the deep bar effect to maintain starting torque while still improving efficiency (89.8% vs 87% for Al).

VI: TRADE STUDY

In an attempt to understand how variations in slot geometry might affect machine performance a short parametric trade was carried out by varying the starting bar diameter from 2 to 10 mm, holding the leakage slot geometry constant, and then varying the leakage slot height from 1 to 5 mm while holding the starting bar diameter at 4.2 mm. The resulting extremes of slot geometry are shown in Fig. 13 and 14.

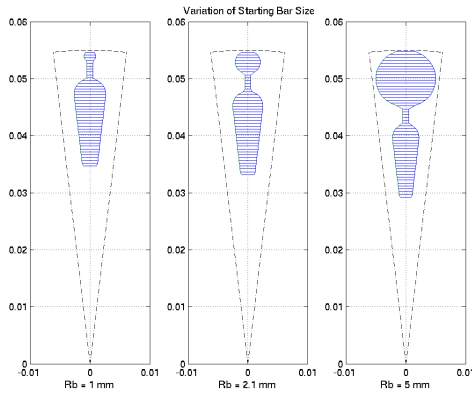


Figure 13: Slot Geometry Varying Starting Bar

Machine performance has been estimated for the ranges of slot geometries shown in Figs 13 and 14, assuming copper to be the cage material. Selected performance parameters are shown in Figs 15 and 16. Fig. 15 shows variation of efficiency and starting torque over variation of starting bar radius, holding the other defining parameters constant.

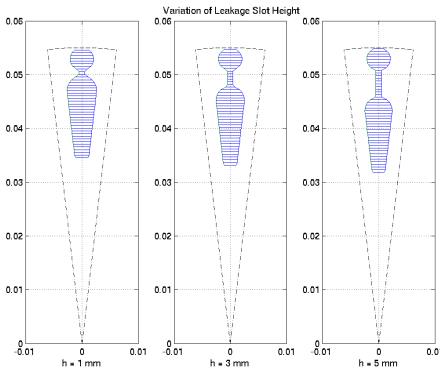


Figure 14: Slot Geometry Varying Leakage Slot Height

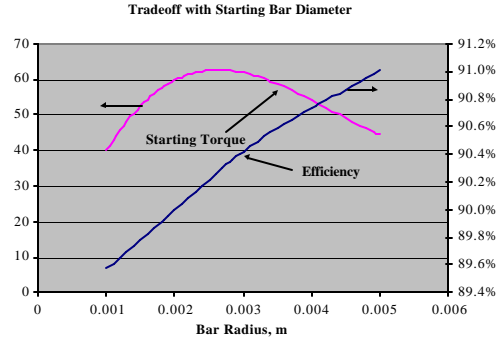


Figure 15: Parametric Study vs. Starting Bar Diameter

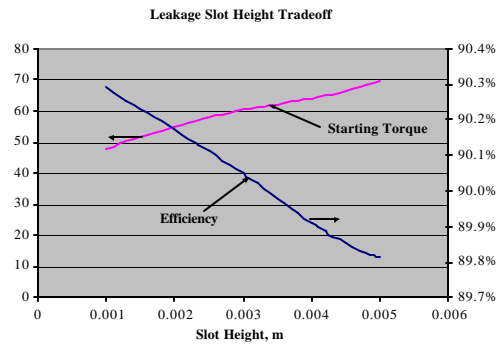


Figure 16: Parametric Study vs. Leakage Slot Height

In the case of leakage bar height there is a tradeoff: increasing the leakage height consistently increases starting torque while also consistently reducing efficiency. This is to be expected as increasing the rotor leakage height pushes the main part of the slot down and reduces available slot width, leaving less conductor in running conditions and increasing running resistance. On the other hand, increasing the starting bar diameter seems to consistently increase efficiency as it increases total conductor available. There is, however, a maximum starting torque at a bar diameter very close to the diameter of the example machine.

VII CONCLUSIONS

This brief study is an attempt to understand how to make appropriate use of different conducting materials in the squirrel cages of cast rotors. In particular, we were interested in how to properly use the higher conductivity of copper in such motors.

As should be clear, the higher conductivity of copper increases skin effect and therefore makes deep bar and multiple cage effects more pronounced. This can be seen from the frequency response plots that examine the impedance per unit length of the rotor slots. High frequency impedance of the rotor slots has an impact on stray load and no-load losses. Medium frequency (around line frequency) impedance effects starting performance. Low frequency impedance (about slip frequency) affects running efficiency. While this has been known for some time, the frequency response plots shown here allow for visualization of these effects. They can tell why a narrow conductor filled slot above the main bar is probably not as effective as a starting bar with a narrower leakage bar below.

We have also confirmed the adequacy of calculating rotor cage impedances using a simple flux tube (one dimensional finite element) model for simple trade studies.

VIII ACKNOWLEDGMENTS

The author would like to acknowledge financial support from the Copper Development Association, provision of data by Dale Peters , Konrad Kundig and John Cowie of the CDA, Dr. E.F. Brush Jr. of BBF Associates and Dr.s R. Kimmich and M Dopplebauer of SEW Eurodrive.

ⁱ Modelling of Rotorbars with Skin Effect for Dynamic Simulation of Induction Machines, J. Langheim, Conference Record, IEEE Industry Applications Society Annual Meeting, 1989, pp 38-44.

ⁱⁱ Induction Machines, Philip Alger, Gordon and Breach, 1970. This is actually an extension to Alger's model, explained in Electric Motor Handbook, H. Wayne Beaty et al. McGraw Hill, 1998

ⁱⁱⁱ Calculation of cage induction motor equivalent circuit parameters using finite elements, S. Williamson, M.J. Robinson, Proc. IEE (Part B) Vol 138, No. 5 pp 264-276, (1991)